

Supplementary Information

Temperature control and particle injection scheme

The temperature of the experimental liquid helium (T_{cell}) is continuously controlled by controlling the pressure of the cell (P_{cell}). To do so, we take advantage of a homemade leak-tight rotating gaseous feedthrough connected to a 300m³/h vacuum pump through a manifold that allows many types of regulations. The main component that we use in these experiments is a diaphragm pressure regulator (throughput 50m³/h) which is an absolute pressure regulator which automatically adapts the pumping speed of the vacuum pump depending on the amount of He that evaporates from the cryostat. The pressure setpoint is given by the pressure inside a reference chamber that we monitor at all times ($P_{\text{regulator}}$). The pressure difference ($P_{\text{regulator}} - P_{\text{cell}}$) is calibrated beforehand and presents a slow drift in time when the stationary state is reached during experimental sessions (maximum temperature drift of 0.7% for a 20-minute session).

To generate the particles that we observe, we inject a gaseous mixture of 98% of He and 2% of H₂ at room temperature directly into the experimental cell through a 1m long and 1.5mm inner diameter cupro-nickel capillary tube. The gas mixture is embedded on the spinning table and newly prepared every day in a 1L reservoir filled at 3.5 bars. To ensure full control over the process, hence repeatability, we have positioned a high-precision single-stage absolute pressure regulator (tied-diaphragm regulator) that sets $P_{\text{injection}}$ on the cupro-nickel capillary tube as close as possible to the entrance into the cryostat's core. This way, we control the end-to-end pressure difference on the injection tube regardless the pressure in the reservoirs (3.5 bars for the first experiment but it decreases injection after injection). The pressure difference ($P_{\text{injection}} - P_{\text{cell}}$) naturally sets the flow rate inside the injection capillary tube.

Figure SI1, shows a typical measurement run. This entire sequence is done under a constant rotation speed. After the first cool down below T_{λ} (lambda point temperature), we bypass the pressure regulation, the temperature rises above the transition, then we inject the particles, trigger the image acquisition and close the bypass of the diaphragm pressure regulator to decrease the temperature. When the fluid transits to its He II phase, the cloud of particles “condenses” onto the vortex lattice. Because solid H₂ is less dense ($\rho_{\text{H}_2}=88\text{kg/m}^3$) than liquid He ($\rho_{\text{He}}=145\text{kg/m}^3$), particles tend to move upwards, out of our region of interest and out of the channel. Therefore, we repeat the cycle described above in order to acquire more data.

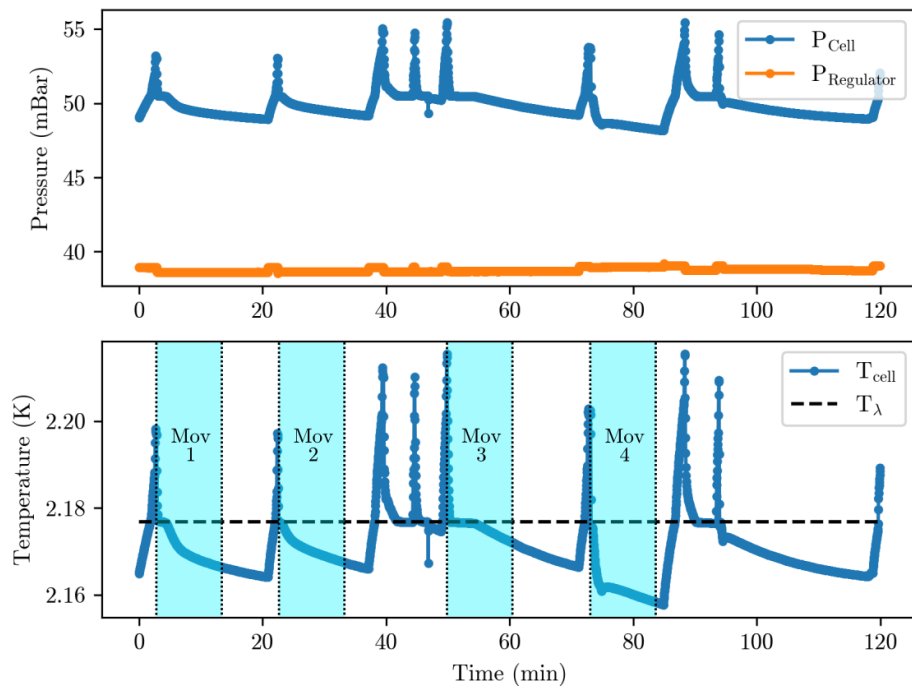


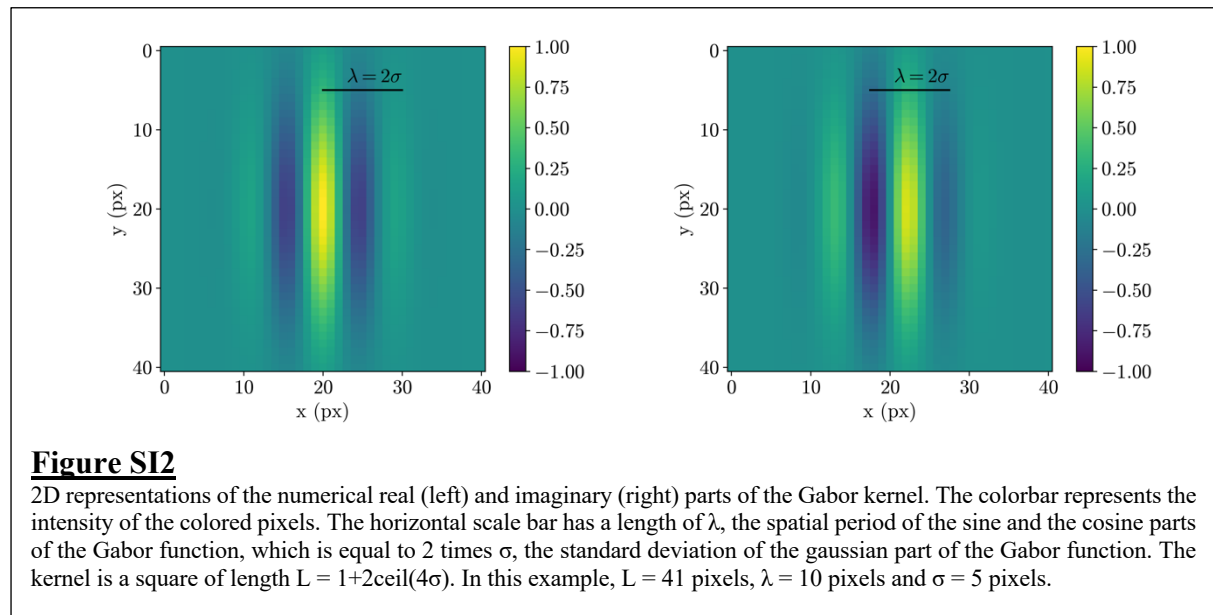
Figure S11

Representation of pressure and temperature during an experimental session. The temperature is dropped by reducing the pressure in the cell (at vapor saturation). Each run starts by injecting H_2 in the cell just above T_{λ} and then opening the regulator valve to allow pumping through it. It can be seen that $P_{\text{Regulator}}$ is slightly lower as the valve is opened, but remains constant during a run. Movies are acquired for 10 to 20 minutes. The next movie has to be taken after re-injecting H_2 as the particles float up and do not stay indefinitely in the region of interest. As seen in the temperature graph, the temperature is not constant during a run, however, the maximum drift is of order 0.7% of the minimum temperature during a run.

Gabor wavelet analysis

To get reliable and trustworthy results, we have conducted many experimental runs. Precisely, we have acquired 500 GB of images which corresponds to about 50000 frames. To analyze this amount of data, we developed an algorithm based on the 2D Gabor wavelet, using Python3 and the OpenCV library. The algorithm was implemented in an embarrassingly parallel manner. The Gabor wavelet is a 2D Gaussian modulated by a complex exponential. We used a simplified form represented on Figure SI2 and defined as followed:

$$G(x, y) = e^{-\frac{(x^2+y^2)}{2\sigma^2}} e^{j\frac{2\pi x}{\lambda}}$$



This expression unveils 3 length scales ordered increasingly: σ defining the Gaussian width, λ defining the probed wavelength, and implicitly L the size of kernel. We have chosen the following relations to link them:

$$\begin{cases} \sigma = \lambda/2 \\ L = 1 + 2 \times \text{ceil}(4\sigma) \end{cases}$$

This definitions allows us to consider that $G(x,y)$ has only one parameter λ . We have simplified the most general form of the Gabor wavelet to respect the vertical invariance and horizontal periodicity of the images that we probe. We use this complex function as a kernel of convolution with our images to compute the amplitude of this correlation at any given point of all our images for many wavelength λ . Then we study the sum of these amplitudes over all the pixels of a given image that we call intensity and we study this intensity as a function of λ .

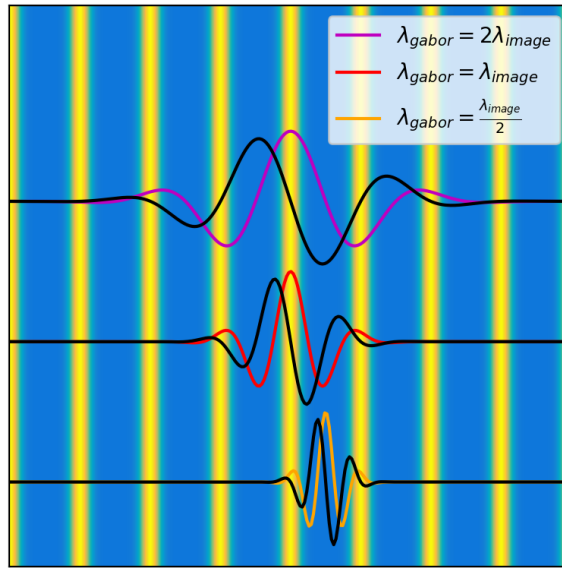


Figure SI3

Superposition of a synthetic image with three Gabor kernels. The lines in black represent the imaginary part of each kernel. λ_{gabor} is the λ discussed in the text and λ_{image} the one of the perfect synthetic image that we intend to measure.

Figure SI3 is here to grasp qualitatively what should we expect from such an image analysis process. The perfect match between the maxima of the kernel and the one of the images in the $\lambda_{gabor} = \lambda_{image}$ case let us conclude that the correlation should be maximum in that case. On the contrary, when $\lambda_{gabor} = 2\lambda_{image}$ the first minima of the kernel falls into a maximum of the probed pattern, one can expect that this negative contribution will annihilate the positive one due to the central pic at order zero. Finally, when $\lambda_{gabor} = \lambda_{image}/2$, the secondary maxima of the kernel matches with local maxima of the image, therefore we should observe a secondary maximum in the amplitude of the correlation. We do this computation in the complex domain in order to get rid of any phase when computing the amplitude of the complex correlation. Moreover, the vertical invariance that we have chosen for the kernel is here to deal with the fact that our images are not as perfect as the synthetic one showed on Figure SI3. Indeed, as seen on Figure 2, the quantum vortices are decorated by irregular point particles. Having a finite vertical extension let the wavelet average the image over a length scale larger than the particles size, which allows particles at different heights to be considered together when looking for a horizontally periodic pattern.

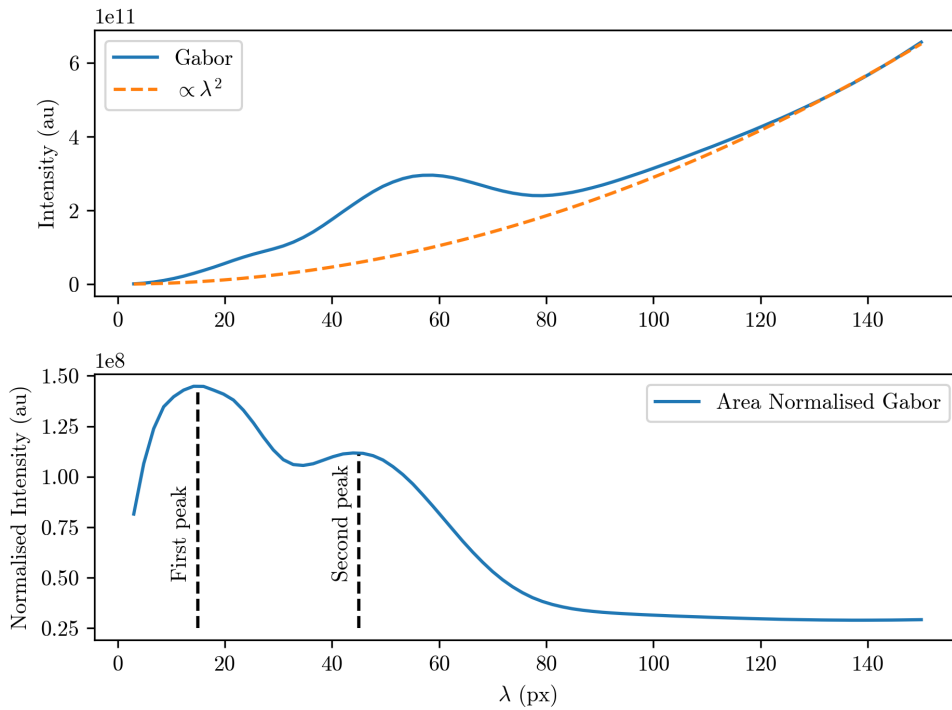


Figure SI4

Intensity and area-normalized intensity signals gathered from a Gabor pass in λ from 1 to 150 pixels large over one image. As seen in the top graph, intensity is asymptotically proportional to λ^2 , and normalizing this signal by λ^2 yields a two-peak signal (bottom). The first peak is the result of multiple contributions, especially particle size, and the second peak holds the information on intervortex distance, as it is directly proportional to the periodicity of the vertical lines in the image.

When computing on an experimental image, we get SI4 (top). One needs to normalize the correlation by the weight of the kernel proportional to λ^2 , that gives the spectrum SI4 (bottom).

We have run several tests on many synthetic images (introducing fake particles and noise) and they all clearly confirm that the second peak corresponds to the periodicity of the pattern. Surprisingly, the first peak after normalization turns out to have a higher normalized intensity. This is because we have not considered in our qualitative analysis that when $\lambda_{\text{gabor}}/2$ approaches the particle size, this should show up in the spectrum. After running a collection of different tests, we can conclude that this first peak is a mixture of $\lambda_{\text{gabor}} = \lambda_{\text{image}}/2$, $\lambda_{\text{gabor}}/5 \cong$ particle size and the particle number density in the image. As our goal is to measure the horizontal periodicity of our images in order to get access to the intervortex distance, we do not push our analysis of the first peak any further. If we were to measure apparent particle size, we would use other methods.

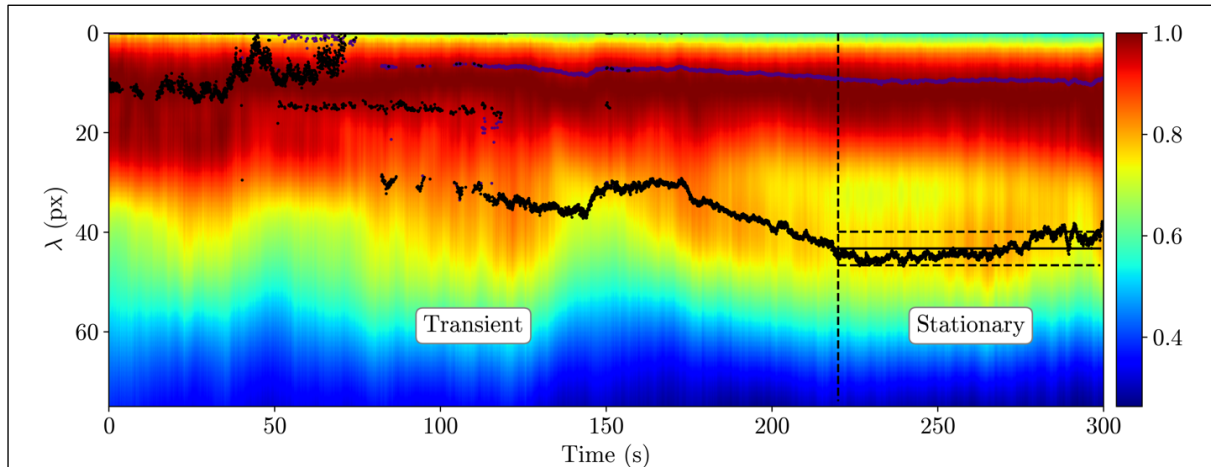


Figure SI5

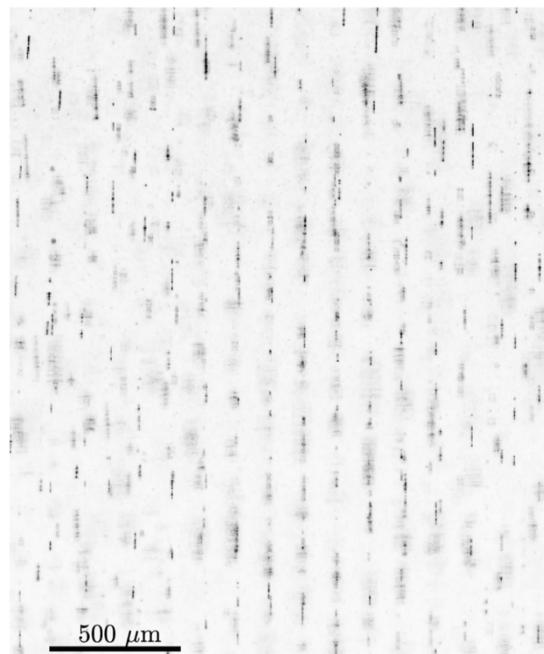
The normalized intensity (Figure SI4 down) are colorcoded and represented as a function of time. The vertical dashed line corresponds to the end of the transient state due to the particle injection scheme. The purple (respectively black) dots are the values of the first (respectively second) peak found at a given time by the bimodal fit we used. The horizontal black line is the average value of the intervortex spacing that we measure, and the horizontal dashed lines represent the standard deviation around it, obtained over the entire stationary dataset at 5RPM.

We have run this analysis on all our images. Using a bimodal fit on each normalized intensity recovered for each frame, we are able to measure the intervortex distance as a function of time with a subpixel resolution. Figure SI5, shows the result of this temporal analysis of a given movie in the 5RPM batch. This representation helps us define when the stationary state is reached and to compute the average and standard deviation of our intervortex spacing measurement. We used this standard deviation alongside the bimodal fit standard deviation to define the vertical error bars in Figure 3.

SI Movie 1: Stability of the vortex lattice

This movie is acquired at a frequency of 25Hz, and is played 4X faster while the cryostat spins at 10RPM. The average velocity of the particles is $20\mu\text{m/s}$ upward. One can also visualize oscillations that have an amplitude of $\sim 50\mu\text{m}$ due to the motion of the He II container with respect to the camera (both on the spinning table). This parasitic motion comes from a misalignment of order $1\mu\text{m}$ between the principal axis of the pumping feedthrough and the axis of rotation of the experiment. This tiny default (when compared to the experiment sizes) is amplified by the 1m lever arm between the body-fixed point of the pumping feedthrough where the HeII container is soldered to the cryostat and our region of interest. These oscillations are deterministic and periodic. This movie demonstrates the stability of the quantum vortex lattice that we observe.

SI_Mov1.mp4



SI Movie 2: Vortex/Vortex interaction and spinning counterflow

This movie is acquired at a frequency of 100Hz with a high-speed camera (20 μ m pixel size) while the cryostat spins at 10RPM, and is played back 4 times slower. We switch on the surface heater at the bottom of the channel with 15mW, corresponding to 37.5 W/m². Shortly after, one can visualize a few hundreds of vortex/vortex interaction events. It is important to stress that these events are triggered by the heating and that the initial condition is well defined. After these strong events characterized by strong accelerations, the particles appear to move mostly upward in a rotating counterflow. Their motion needs to be further characterized in order to search for signs of their interactions with the polarized quantum vortex tangle (out of scope of this paper).

SI_Mov2.mp4

